Controlled Delivery of Krypton-81m Boli in Normal Subjects: Results and Implications

Sylvia Verbanck, Sujatha Koneru, Miles Cohen, Stewart W. Clarke and John E. Agnew

Medical Physics and Thoracic Medicine Departments of the Royal Free Hospital and School of Medicine, London, United Kingdom

Interregional sequential filling potentially affects lung ventilation imaging, depending on the distribution of the tracer within the inspired volume. We investigated its importance quantitatively under near tidal breathing conditions in the upright lung using a short-lived radioactive tracer. Ten normal volunteers performed two runs of 900-ml breaths (from functional residual capacity) in which 100 ml of ^{81m}Kr boli were delivered "early" or "late" in inspiration, i.e., 50 ml or 450 ml volumetric depth. Apex-to-base gradients in the vertical profile were -106 ± 22 (s.e.) counts/cm (early) and -187 ± 24 (s.e.) counts/cm (late). Ratios of upper-to-lower regional ventilation (U/L) were 0.88 ± 0.01 (s.e.) (early) and 0.81 ± 0.01 (s.e.) (late). Simulations with a compartment model show that a simple pattern of sequential filling can by itself account for the experimental results observed. Control over ^{81m}Kr delivery can be important to physiologically accurate assessment of ventilation-perfusion matching. Controlled delivery techniques could also modify effectiveness and targeting of other inhaled agents including therapeutic aerosols.

J Nucl Med 1993; 34:1859–1865

Vertical activity profiles of lung images obtained with inhaled radioactive tracers can be influenced by gravity-dependent ventilation distribution between upper and lower lung regions. The quantitative implications of the effect will vary with the inhalation mode adopted. Although sequential filling between upper and lower lung regions has been implicated as a possible contributory factor to differing vertical activity distributions in comparative trials of ventilation imaging agents (aerosols and gases), the quantitative contribution of sequential filling to clinical imaging studies has been less clearly established. We aimed to assess the extent to which this mechanism—rather than any other aspect of lung inhomogeneity—influences tracer distributions under near tidal breathing conditions in upright normal subjects.

The nature of interregional inhomogeneity of ventilation has long been understood. In the 1960s, it was demonstrated that for lung volumes above functional residual capacity (FRC), lower lung regions were smaller in volume, but received a larger portion of the inspired air (*1*) and that this phenomenon was gravity-dependent (*2*). These authors introduced the "onion-skin model" representing regional volume as a function of total lung volume for various lung heights (*1,2*). For volumes above FRC, this was reported to be a linear function, so that the proportion of inspired air to top and to bottom lung regions was independent of lung volume, i.e., no interregional flow sequencing.

In the early 1970s, experimental evidence was provided for the existence of interregional flow sequencing during inspiration as well as expiration (*3–5*). Anthonisen et al. (*5*) suggest actual values of curvilinear deviation from the linear onion-skin model in normal subjects during "slow" breathing (i.e., flows < 1 liter/sec). Pedley et al. (*6*) modeled regional volume distribution on the basis of physiological values of compliance and airway resistance. Their results suggest that the flow sequencing values of Anthonisen et al. (*5*) may well overestimate the real situation.

The changing relative contribution of resistance and compliance to regional flows as lung volume increases is probably the most important mechanism underlying sequential filling in normal subjects sitting upright. However, for normal subjects in the supine position (*7*) and for patients with various pulmonary diseases, an alternative mechanism of sequential filling occurs: basal airway closure at low volumes and the progressive recruitment of these airways during inspiration. In the present study, subjects, sitting upright, were instructed to breathe from FRC. Basal airway closure is therefore expected to be minimal at all lung volumes involved.

For this investigation into the implications of the overall sequential filling pattern for ventilation imaging, we made use of the short-lived radioactive tracer krypton-81m (^{81m}Kr) which has a 13.4-sec half-life. The experimental part of the study covers the controlled delivery of ^{81m}Kr boli relatively early or late within the inspired volume. The experimental results are then set against computed simulations of the ^{81m}Kr washin maneuver. For these simulations, we devised a simple compartment model incorporating published regional flow and volume distribution data.

Received Jan. 26, 1993; revision accepted June 23, 1993.
For correspondence and reprints contact: Dr. S. Verbanck, Medical Physics Dept., Royal Free Hospital, Pond St., Hampstead, London NW3, United Kingdom.

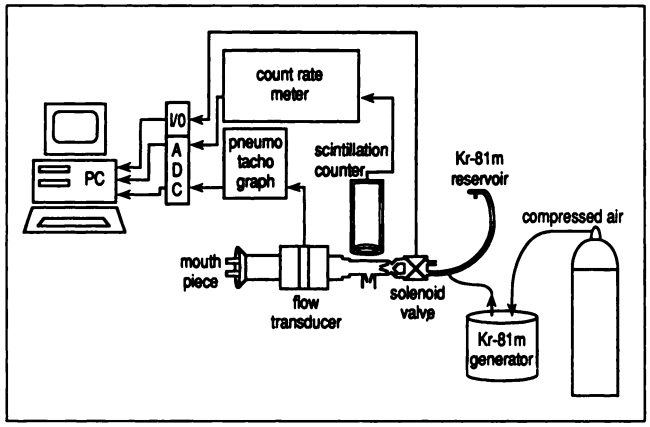

FIGURE 1. Schematic representation of the experimental setup. While seated in front of a LFOV gamma camera (not represented in the figure), the subjects breathe from the mouthpiece, while watching the computer screen.

MATERIALS AND METHODS

Experimental Setup

Figure 1 schematically shows the breathing assembly with three main elements, connected to a computer via analog-to-digital converter and input/output devices to record and control the experimental procedure. A pneumotachograph (Fleisch type), a scintillation counter with a NaI(Tl) crystal 5 cm in diameter and a solenoid valve (Sirai pinch tube type) were used. A turbopascal program was developed to coordinate the experimental procedure (including calibration) and to store the recorded volumes and count rates as a function of time every 0.05 sec at the end of each run.

A mouthpiece was connected via the pneumotachograph to a T-piece with two one-way valves in order to separate the inspiratory from the expiratory pathway. A well-collimated scintillation counter was placed to detect the actual ^{81m}Kr profile in the inspired volume, as well as the ^{81m}Kr contents on expiration along a pathway section common to inspiration and expiration. In order to minimize dead space, the equipment design had to be compact and the counter could not be totally shielded from activity in the ^{81m}Kr reservoir or in the subject's lungs. However, the aim was merely to verify the presence of a count rate peak in the inspired volume, and the absence of a well-defined peak in the expired volume (see RESULTS).

At the end of the inspiratory pathway, a Y-piece allows for gas supply from two soft tubings, fixed in a solenoid valve unit. The solenoid valve provides occlusion, or alternatively an open pathway to room air and the ^{81m}Kr reservoir, respectively, with a response time of ±45 msec upon activation from the computer program. The total instrumental dead space (taken as the volume between the reservoir and the mouthpiece) was 75 ml. The ^{81m}Kr reservoir was an anaesthetic "elephant tube" (1 m in length) with a 1-mm bore inlet and outlet at its two extremes. The inlet received the ^{81m}Kr from the generator capillary, through which air was flushed at 1 liter/min.

Experimental Procedure

The assembled apparatus was mounted on a trolley that could be adjusted to a comfortable patient position with respect to the gamma camera (LFOV Ohio/Nuclear, Solon, OH). The patients sat upright leaning against the gamma camera to record posterior images. While performing the ^{81m}Kr runs, the gamma camera recorded a static lung image until it had cumulated a total of 200 kcounts (after approximately 1 min depending on the generator activity).

With a nose clip on, the patient performed the following sequence of maneuvers. First, the patient breathed normally through the mouthpiece for 1 min, during which time the ^{81m}Kr was allowed to build up in the reservoir (unless otherwise stated, the valve is open to air in order to isolate the ^{81m}Kr reservoir from the circuit). Then, the patient took three more tidal breaths; an inspiration to total lung capacity, an expiration to residual volume and a final inspiration to reach FRC. At this lung volume, the patient held his breath for approximately 2 sec, while the pneumotachograph, PC computer and gamma camera initiated the actual maneuver. Aided by the on-line volume trace on the PC monitor, the patient was instructed to breathe in a sawtooth manner in between two lines. The reference level was drawn to represent FRC (shown later in Fig. 4A as level 0), and a second line appeared 900 ml above the reference level.

This sequence of maneuvers was practiced at least twice without any ^{81m}Kr in the reservoir to make the patient comfortable with the experimental procedure. After this proved satisfactory, we proceeded with the "early" and "late" ^{81m}Kr delivery runs in randomized order with approximately 5 min in between each run.

In the early run, the software was set to make the valve release the ^{81m}Kr from the reservoir with a delay volume of 50 ml above the reference level corresponding to FRC. In the late run, the delay volume was 450 ml. In either case, the computer switched the valve to air again 100 ml after the release of the bolus, closing off the reservoir where ^{81m}Kr builds up until its release in the subsequent breath.

Data Analysis

The static lung images (64 × 64 pixels, 7 mm × 7 mm each) were analyzed as follows: vertical distribution of count rate (i.e., "ventilation" as assessed with ^{81m}Kr) was expressed as a 64-point vertical profile obtained by adding left and right lung profiles (excluding activity in the trachea). These vertical profiles were smoothed once (1:2:1 weighted smooth) and normalized to a total profile count of 200,000 counts. Because of the high signal-to-noise ratio, no background correction was applied.

For the evaluation of parameters that assess the gravity-dependent regional ventilation, the normalized vertical lung profile was truncated at the top and bottom of the lung where count rates were less than 30% of the peak count rate in that profile. The height of the lung will be referred to as the real size length (in centimeters) between the top and bottom of the truncated lung profile.

We chose following two parameters to represent apex to bottom distribution of ventilation (Fig. 2):

1. U/L: the ratio of average count rate in the upper (U) and lower (L) regions, obtained by splitting the lung profile into two parts of equal height.
2. S: the slope of the regression line, computed from the middle part of the vertical profile. The profile was subdivided in three parts of equal height; the middle of these was used for regression analysis resulting in regression slopes S (i.e., ventilation gradients in counts/cm).

Model Description

For the simulations of the experiments, we used a compartment lung model similar to the one described by Verbanck and Paiva (*8*). Two alveolar compartments represent upper and lower

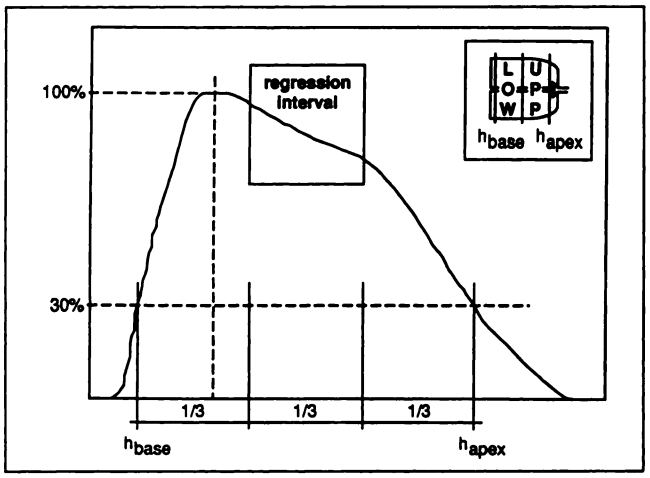

FIGURE 2. A typical vertical profile of count rate over the entire lung of a normal subject to illustrate the computation of parameters S (apex-to-base countrate gradient over the middle third of the profile) and U/L (ratio of upper to lower count rate). See text for details.

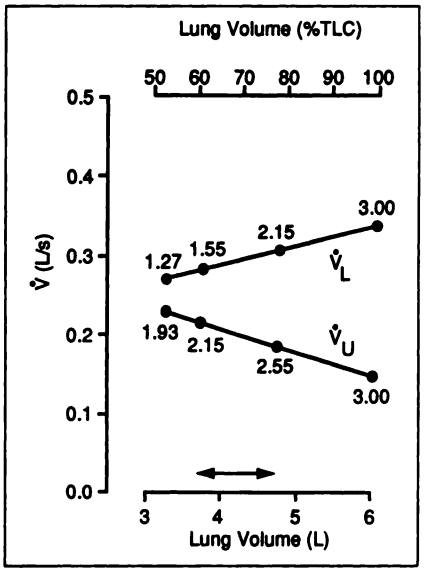

FIGURE 3. Regional flow distribution during inspiration and expiration between overall lung volumes 3 liters and 6 liters. $\dot{V}_U$ and $\dot{V}_L$ are flows to upper and lower lung region, respectively; $\dot{V}_U + \dot{V}_L$ = 0.5 liters/sec at all times. The dots on the regional flow lines indicate alveolar lung volumes of the corresponding region at overall alveolar lung volumes 3.2 liters, 3.7 liters (=FRC), 4.7 liters and 6 liters; note that for 6 liters, both upper and lower lung region are considered equally expanded to 3 liters.

lung regions. At FRC, the upper lung volume is approximately 50% larger than the lower. Instrumental and anatomical dead space down to the first generation beyond the trachea is common to both alveolar compartments and amounts to 120 ml. The remaining conducting airways that lead to each alveolar compartment are treated as regional dead space compartments of 45 ml each.

Equations describing the soluble and insoluble gas concentration in each model compartment during a given respiratory maneuver are described in detail by Verbanck and Paiva (*8*). When solved with a finite difference method (time step 0.001 sec), these equations describe convective gas flow into each homogenously, isotropically expanding alveolar compartment, assuming instantaneous mixing of inspired and resident gas at every time step. The equations for an insoluble gas were adapted for ^{81m}Kr simply by adding a term accounting for the radioactive decay.

Overall inspiratory and expiratory flows are considered to be constant at all lung volumes (volume is taken to be a sawtooth function of time). The contribution of regional flow into either upper or lower compartments varies as a function of total lung volume as illustrated in Figure 3. This extent of interregional flow sequencing, given by the slope of the flows to upper and lower compartment ($\dot{V}_U$, $\dot{V}_L$) as a function of lung volume, was previously used by Verbanck and Paiva (*9*), based on Anthonisen et al. (*5*), for quantitative evaluation of interregional contribution to overall lung ventilation inhomogeneity.

Figure 3 shows that for the maneuver performed here (900-ml tidal breathing from FRC) the volume ratio of lower-to-upper volume is 0.72 at FRC. While the overall flow is 0.5 liter/sec at all lung volumes, the ratio of average flow-to-lower and upper region ($\dot{V}_L/\dot{V}_U$) over a breath of 900 ml from FRC is 1.5, i.e., the smaller (lower) region is ventilated more than the larger (upper) region. It can also be inferred from Figure 3 that the late bolus inspired at the end of a 900-ml inspiration from FRC will be more inhomogeneously distributed between upper and lower alveolar compartments than the early bolus coming into the lung just above FRC.

RESULTS

We studied 12 normal volunteers who gave informed consent prior to the study, which was approved by the hospital's ethical practices subcommittee. In Table 1, lung function parameters are listed for all 12 subjects, but the average values (lower line) represent the mean value of the first 10 subjects. Subject SA was excluded from further data analysis because he failed to comply adequately with the breathing maneuver (he demonstrated a progressive decrease of end-tidal lung volume). Subject WB was discarded because the late bolus was not completely inhaled into the alveolar space, as inferred from the ^{81m}Kr bolus reappearance at the beginning of expiration. In the remaining 10 subjects, average tidal volume was 937 ± 91 (s.d.) ml and average flow was 480 ± 77 (s.d.) ml/sec. The intrasubject variability of volume during each run as measured by the coefficient of variation was less than 10% in all subjects. The difference in average flow between the early and late run was always less than 15%.

Figure 4 shows for subject BD, the volume and ^{81m}Kr scintillation counter tracings produced during an early and a late run and the corresponding total lung vertical profiles recorded by the gamma camera. It demonstrates the rationale for having a scintillation counter viewing the tubing where inspiratory and expiratory flows pass. This provides a means of ensuring that the computer-controlled ^{81m}Kr release functions correctly (e.g., no obstruction of tubing between the ^{81m}Kr generator and the breathing circuit) and that it genuinely generates a bolus (reflected by a 100-ml-wide peak). Similarly, the absence of a peak in the expiratory part of the scintillation counter trace clearly indicates if late bolus delivery to the alveolar lung zones has failed, as was the case for one subject (WB).

TABLE 1
Lung Function for 12 Subjects Performing the Early and Late Krypton-81m Bolus Washin*

No.	Subject	Age (yr)	Weight (kg)	Height (cm)	FEV1 (%Predicted)	TLC (liter)	FRC (%TLC)	RV (%TLC)
1	CG	34	66	171	98	5.7	61	28
2	RD	30	56	163	86	5.1	56	29
3	FJ	30	48	168	90	5.4	55	28
4	SP	26	60	162	108	5.5	74	41
5	GD	34	42	152	97	4.2	60	29
6	DM	28	85	188	113	8.4	58	22
7	TJ	37	84	161	107	5.3	43	24
8	BD	40	58	175	114	7.7	48	29
9	CC	35	67	183	116	8.6	61	32
10	BR	36	61	161	100	4.7	45	28
Average		32	60	170	105	6.3	57	28
11	SA	31	68	174	105	6.5	69	29
12	WB	27	88	179	128	8	50	22

*Average of 10 subjects for whom the test was successful.
FEV1 = forced expiratory volume in liters; RV = residual volume; and TLC = total lung capacity.

Results for the 10 subjects with valid data are summarized in Figure 5 (left panel: ventilation ratio U/L, right panel: regression slope S). Corresponding model simulations are shown in Table 2. These represent simulations of the experimental procedure followed here, i.e., 937-ml tidal breaths from FRC (=3.7 liters) with an average flow of 0.5 liter/sec. The 100-ml ^{81m}Kr boli are simulated 50 ml (early) and 450 ml (late) after the onset of inspiration. Assuming a summed instrumental and anatomical dead space of 210 ml, these boli reach the alveolar compartments after 260 ml and 660 ml of inspired air. Details of the three simulations carried out are:

Simulation 1: Regional volume and flow parameters as shown in Figure 3 (lower-to-upper lung volume ratio is 0.72; $\dot{V}_L/\dot{V}_U = 1.5$).

Simulation 2: Regional volume distribution at FRC is more homogeneous than in Figure 3 (lower-to-upper lung volume ratio changes to 0.80).

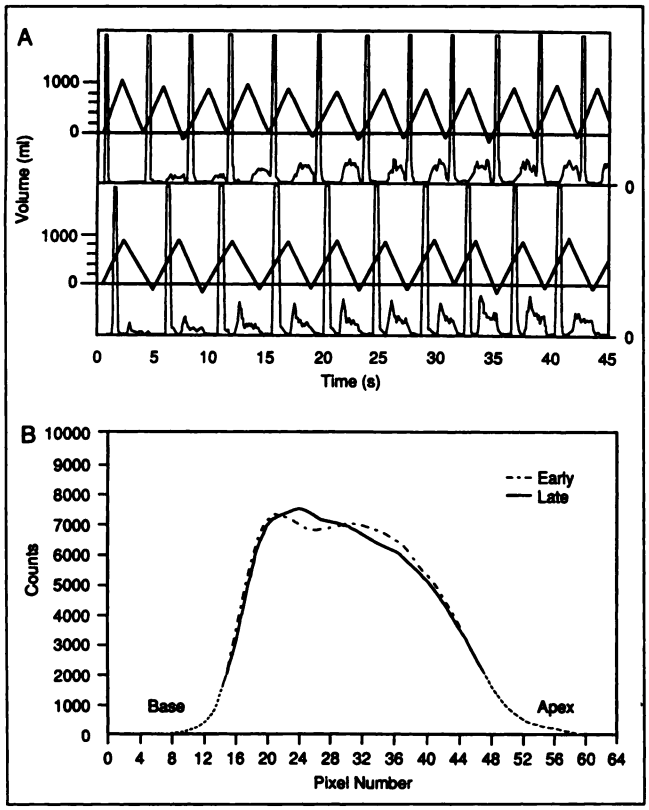

FIGURE 4. (A) Heavy solid lines represent a 45-sec recording of volume (from the pneumotachograph) in milliliters during bolus delivery "early" (above) and "late" (below) in each inspiration; the volume level corresponding to FRC was handled by the computer as a reference level for controlling the release of the boli. Light solid lines are the corresponding vertical count rate profiles (from the scintillation counter) in arbitrary units which show boli during each inspiration and expiratory traces that reflect the progressive build-up of krypton in the lung. (B) Vertical count rate profiles resulting from the maneuvers depicted in (A).

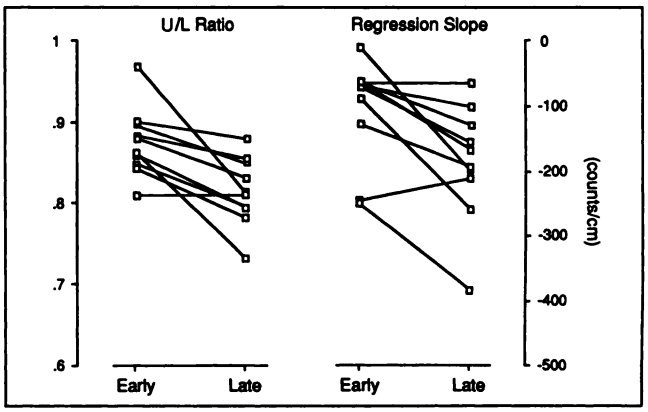

FIGURE 5. Experimental values of parameters U/L and S resulting from "early" and "late" bolus delivery in the first 10 normal subjects listed in Table 1. For both the U/L ratio and the regression slope, the difference between "early" and "late" bolus delivery is statistically significant ($p < 0.01$, Wilcoxon matched pairs signed rank test).

TABLE 2
Model Simulations

	Model parameters		Model simulation U/L values	
	Volume ratio	Flow* sequence	Early bolus	Late bolus
Simulation 1	0.72	A	0.92	0.83
Simulation 2	0.82	A	0.90	0.80
Simulation 3	0.72	B	0.92	0.87

*Flow sequence pattern A is the one depicted in Figure 3, whereas pattern B results from halving the slopes of regional flow to upper and lower alveolar compartment.

Simulation 3: Interregional flow sequencing is smaller than in Figure 3 (the slopes of $\dot{V}_U$ and $\dot{V}_L$ as a function of lung volume are halved, the average $\dot{V}_L/\dot{V}_U$ ratio is maintained at 1.5).

DISCUSSION

This study shows that in normal upright subjects vertical distribution of ventilation significantly depends on whether the radioactive tracer ^{81m}Kr is inhaled early or late in each inspiration (Fig. 5). Overall, ^{81m}Kr distribution tends to follow that of ventilation (*10*). Our results quantitatively demonstrate the extent to which distribution within the inspired volume can affect indices of regional ventilation distribution.

The absolute value of apex-to-base gradient (S) increases by 76% when the ^{81m}Kr bolus is delivered 400 ml deeper in the inspired volume; the corresponding increase of U/L was 8%. The latter parameter allows a particularly straightforward comparison with the simple compartment model we devised to test the extent of interregional flow sequencing. The experimentally observed differences in U/L between early and late bolus are within the range of those predicted by model simulations with realistic regional volume and flow distributions between upper and lower lung regions (Simulations 1–3 in Table 2).

The reason for carrying out three simulations instead of just one with a given set of regional volume and flow parameters is due to the variability of these parameters demonstrated in the existing literature (*11*). Also, most published reports only specify approximate flow ranges within which the regional volume data may be considered valid. Regional volume and flow distributions are known to be very sensitive to flow even within these flow ranges (*4,12,13*). Thus, precise parameter fitting of the model in order to perfectly match simulated and experimental U/L would have been inappropriate. With respect to Simulation 1, Simulation 2 shows the effect of a more homogeneous distribution of lower and upper regional volume at FRC, whereas Simulation 3 shows the effect of halving interregional flow sequencing. The value of the three model simulations taken together (Table 2) lies in the general demonstration that the differences between upper and lower ratios in early and late boli delivery can be accounted for by interregional flow sequencing.

Our model makes no steady-state assumptions in that our initial condition is zero activity in the lung. By contrast, Valind et al. (*14*) used a similar compartmental model (ventral, middle, and dorsal instead of upper and lower) for the simulation of a steady state in order to estimate regional ventilation according to the method proposed by Fazio and Jones (*15*), and evaluate the estimation errors. We took into consideration the conclusion of Valind et al. (*14*) that the dead space markedly affects the estimated ventilation distribution and incorporated instrumental as well as anatomical dead spaces in our model for the nonsteady-state simulations.

As part of a critical investigation into the validity of the steady-state method, Amis and Jones (*16*) compared the apex-to-base count distribution obtained by inspiring a bolus early in inspiration (as achieved by their mouthpiece method) with respect to a quasi-uniform ^{81m}Kr-labeled-inspired volume. Although provisions have to be made for the apparent difference in tidal volume and possible difference in flow (not specified) between the two experiments, the bolus seemed to be distributed more to the lung apex with respect to the evenly inspired volume. Their results are in line with our finding that a relatively early delivered bolus shows a larger apex-to-base count ratio than a relatively late bolus.

Some previous work on ^{81m}Kr delivery early or late in inspiration involved injecting the boli at different volumetric depths with respect to the mouth (*17,18*) using a delay tube to make the difference between early and late bolus delivery. However, as was pointed out by Grant et al. (*4*), the use of a tube to function as a delay volume leads to important differences in dispersion of early and late boli during their transport to the lung units over which they are distributed. Our setup which delivers the boli at the same site but at a different time (Fig. 1), avoids this problem. Moreover, the continuous recording of volume and flow throughout the experimental procedure allows for a better control of the variables by which the comparison between early and late bolus delivery is so crucially affected. In the previous studies, no account was made for eventual differences between volume and flow in early relative to late bolus delivery.

Our early U/L are close to previously reported experimental values by Mostafa et al. (*19*), who found U/L = 0.85 with a reservoir system, approximately corresponding to our early bolus mode and Mohsensifar et al. (*20*), from whose data we derive U/L = 0.87, also with a ^{81m}Kr delivery system similar to our early bolus mode. In fact, with the most commonly used ^{81m}Kr U-tube ("reservoir") delivery system, ^{81m}Kr is predominantly inhaled early in inspiration, whatever the tidal volume, due to low volumetric flow rates from the generator into the delivery reservoir.

Our adaptation of the U-tube type of ^{81m}Kr delivery

system proved to provide a satisfactory means of delivering ^{81m}Kr boli at predetermined depths in the inspired volume (Fig. 4A). Any such adaptation requires the following considerations:

1. Sufficient air volume following the bolus (in our case 900 ml–450 ml–100 ml = 350 ml). Depending on the patients' anatomical dead space, the transit of the ^{81m}Kr bolus through the instrumental and anatomical dead space cannot be completed and its distribution over the alveolar space is not fully achieved. This is what happened in patient WB.
2. Comparable flow conditions in early and late bolus delivery, which may call for the incorporation of flow restrictors in the inhalation apparatus. In our experiments, the relatively narrow pinch holes of the valve serve the purpose of flow restrictors.
3. Comparable dispersion of bolus on its way through the instrumental dead space by a release of the bolus at the same location in the instrumental dead space at different stages (different times) in the inspiration, in contrast to what is achieved by simply inserting a tube to function as a delay volume.

Our results show that control over ^{81m}Kr delivery is important to using this gas for ventilation distribution measurements, e.g., in combination with the perfusion counterpart. They do also, at least in part, account for vertical distribution differences reported in comparable studies between different ventilation agents (gases or aerosols). Finally, they carry implications for the regional targeting of ventilation agents in the diagnostic procedure and the localized delivery of therapeutic aerosols. We will further discuss each of these aspects.

Ventilation-Perfusion Relationships. Regional ventilation-perfusion studies can be quantitated by the V-Q difference (*21*) rather than the V/Q ratio (*22*). The index used by Vernon et al. (*23*) was a measure of deviation of V-Q curves from a range of V-Q curves obtained from a normal population. Its merit was shown by a very good correlation with FEV_1(%predicted) in 25 asthmatics (*23*). It is noteworthy that our differences between early and late ventilation profiles are of the same magnitude as the differences which differentiated between normal and abnormal patients in the study by Vernon et al. (*23*).

Without careful control over inhalation conditions relevant to flow sequencing effects (lung volume and activity distribution within the inspired volume), such effects could potentially introduce an artifact into the V-Q analysis. Conversely, strict control over inhalation conditions could potentially maximize the value of V-Q analysis.

Comparison of Different Ventilation Agents. When comparing vertical distributions obtained with different ventilation agents, three sources of differences are to be taken into account: (1) distribution of activity over the inspired volume; (2) the maneuver (i.e., shallow or deep inhalations, number of breaths); and (3) physical properties of the tracer (gas or aerosol radioactive half-life). The present study was designed to systematically investigate the first aspect in normal subjects under controlled conditions.

Additional factors may of course arise in patients with airway disease. However, differing activity distribution within the inspired volume may well have contributed to reports of smaller apex-to-base activity gradients for ^{81m}Kr than for radio-aerosols such as ^{99m}Tc-DTPA or Technegas (*24–27*). Our study suggests that at least part of this difference could be explained by the sequential filling of the lung, the ^{81m}Kr being delivered early in inspiration whereas the aerosols are more homogeneously spread over the entire inspired volume. From the viewpoint of flow sequencing, a more evenly distributed ventilation agent over the tidal volume corresponds to a centrally delivered bolus. The gravity-dependent nature of these differences in vertical gradients is further confirmed by the similar apex-to-base gradients observed when patients are delivered ^{81m}Kr or ^{99m}Tc in the supine position (*28*).

Diagnostic Potential. It may sometimes be appropriate to try to optimize control over regional distribution of a ventilation imaging agent. For instance, Alderson et al. (*29*) suggested that ventilation-perfusion mismatch assessment can be most effective when the patient inhales the ventilation agent while supine in order to minimize the apex-to-base gradient. When a perfusion image indicates a questionable defect in the basal lung zone, basal targeting of the ventilation could be enhanced by delivering ^{81m}Kr relatively late in inspiration.

When patients are imaged in the supine position, dependent (posterior) airways may remain closed even at relatively high lung volumes (*2*). Even for normal supine subjects, Engel and Prefaut (*7*) have suggested that flow sequencing due to progressive opening of closed airways may affect ventilation distribution over the volume range 40%–80% of vital capacity. For asthmatic subjects, it has been suggested that vertical gradient differences between ^{81m}Kr (i.e., early bolus) and DTPA aerosol (evenly distributed activity) could be due to a substantial proportion of closed airways at volumes close to FRC (*29*).

It seems unlikely that imaging techniques could be readily manipulated to yield clinically useful regional mapping of airway closure sites. Nevertheless, one report (*18*) has claimed that ^{81m}Kr boli delivered either early or late in inspiration would distinguish different types of pulmonary diseases. This speculation would need to be tested with excellent control over flow and volume variables, but does imply that differing forms of pulmonary diseases may specifically affect flow sequencing and thereby vertical ventilation distribution of ventilation agents.

Therapeutic Targeting. Effective targeting of therapeutic aerosols could also benefit from a more controlled delivery into a given inspired volume: a drug would be delivered as a late bolus to a patient who needs targeting towards a disease process predominantly affecting the basal lung region. This suggestion obviously rests on the hypothesis that the interregional aerosol distribution follows the gas interregional distribution. Clearly this will less readily oc-

cur when the particle size is large (>2 μm) as deposition by impaction (flow rate dependent) will lessen the particles' ability to follow gas pathways to the periphery. Model simulations by Scott and Taulbee (*31*) predict a larger absolute apex-to-base gradient of 1-μm particle deposition with respect to the tidal volume distribution. However, the experimental results of Chamberlain (*32*), comparing images obtained with ^{133m}Xe and 0.8 μm of ^{99m}Tc-labeled aerosols (both agents were evenly spread over the inspired volume), found very similar vertical lung profiles indicating the potential for parallels between small particle and gas distribution patterns.

CONCLUSION

Krypton-81m has important potential for quantitative, physiological assessment of regional ventilatory distribution. To awaken it from its current perceived role of "sleeping genie" (*33*), techniques are appropriate which control its distribution within the inspired volume. Therefore, we can hope to better assess the quantitative significance of the physiological factors which influence regional ventilation. The modeling simulations reported in this paper were deliberately simple. They demonstrate that very straightforward flow sequencing modeling concurs well with experimental observation. Our data help to indicate the extent to which selective apical or basal targeting of inhaled agents may be feasible.

ACKNOWLEDGMENTS

The authors thank Dr. M. Paiva for his advice during the preparation of this manuscript. This work was supported by a fellowship from the Commission of the European Communities.

REFERENCES

1. Milic-Emili J, Henderson JAM, Dolovich MB, Trop D, Kaneko K. Regional distribution of inspired gas in the lung. *J Appl Physiol* 1966;21:749–759.
2. Kaneko K, Milic-Emili J, Dolovich MB, Dawson A, Bates DV. Regional distribution of ventilation and perfusion as a function of body position. *J Appl Physiol* 1966;21:767–777.
3. Clarke SW, Jones JG, Glaister DH. Change in pulmonary ventilation in different postures. *Clin Sci* 1969;37:357–369.
4. Grant BJB, Jones HA, Hughes JMB. Sequence of regional filling during a tidal breath in man. *J Appl Physiol* 1974;37:158–165.
5. Anthonissen NR, Robertson PC, Ross WRD. Gravity-dependent sequential emptying of lung regions. *J Appl Physiol* 1970;28:589–595.
6. Pedley TJ, Sudlow MF, Milic-Emili J. A nonlinear theory of the distribution of pulmonary ventilation. *Respir Physiol* 1972;15:1–38.
7. Prefaut CH, Engel LA. Vertical distribution of perfusion and inspired gas in supine man. *Respir Physiol* 1981;43:209–219.
8. Verbanck S, Paiva M. A theoretical basis for the 'time 0' correction. *J Appl Physiol* 1993: in press.
9. Verbanck S, Paiva M. Model simulations of gas mixing and ventilation distribution in the human lung. *J Appl Physiol* 1990;69:2269–2279.
10. Lythgoe MF, Davies H, Kuba A, Toth-Abonyi M, Gordon I. Can dynamic Krypton-81m imaging separate regional ventilation and volume? *J Nucl Med* 1992;33:1935–1939.
11. Hughes JMB, Amis TC. Regional ventilation distribution. In: Engel LA, Paiva M, eds. *Gas mixing and distribution in the lung*. New York: Marcel Dekker; 1985.
12. Bake B, Wood L, Murphy B, Macklem PT, Milic-Emili J. Effect of inspiratory flow rate on regional distribution of inspired gas. *J Appl Physiol* 1974; 37:8–17.
13. Connolly T, Bake B, Wood L, Milic-Emili J. Regional distribution of a ^{133}Xe-labeled gas volume inspired at constant flow rates. *Scand J Resp Dis* 1975;56:150–159.
14. Valind SO, Rhodes CG, Jonson B. Quantification of regional ventilation in humans using a short-lived radiotracer: theoretical evaluation of the steady state model. *J Nucl Med* 1987;28:1144–1154.
15. Fazio F, Jones T. Assessment of regional ventilation by continuous inhalation of radioactive krypton-81. *Brit Med J* 1975;3:673–676.
16. Amis TC, Jones T. Krypton-81m as a flow tracer in the lung: theory and quantitation. *Bull Eur Physiopath Resp* 1980;16:245–259.
17. Uren NG, Davies SW, Agnew JE, et al. Reduction of global ventilation-perfusion mismatch on exercise is related to exercise capacity in chronic heart failure. *Cardiology* 1991;84:(suppl) II-7.
18. Kurosawa H, Matsubayashi S, Ishii Y, et al. *Kaku-Igaku* 1990;27:125–131.
19. Mostafa AB, Childs PO, Williams NR, Causer DA. Regional pulmonary distribution of krypton-81m gas delivered by different breathing systems. *J Nucl Med* 1985;26:191–193.
20. Mohsenifar Z, Ross MD, Waxman A, Goldbach P, Koerner SK. Changes in distribution of lung perfusion and ventilation at rest and during maximal exercise. *Chest* 1985;3:359–362.
21. Burton GH, Vernon P, Seed WA. An automated quantitative analysis of ventilation-perfusion lung scintigrams. *J Nucl Med* 1984;25:564–570.
22. West JB. *Regional differences in the lung*. In: West JB, ed. New York: Academic Press; 1977:202–208.
23. Vernon P, Burton GH, Seed WA. Lung scan abnormalities in asthma and their correlation with lung function. *Eur J Nucl Med* 1986;12:16–20.
24. James JM, Herman KJ, Lloyd JJ, et al. Evaluation of ^{99m}Tc Technegas ventilation scintigraphy in the diagnosis of pulmonary embolism. *Br J Radiol* 1991;64:711–719.
25. Agnew JE, Francis RA, Pavia D, Clarke SW. Quantitative comparison of ^{99m}Tc aerosol and ^{81m}Kr ventilation images. *Clin Phys Physiol Meas* 1982; 3:21–30.
26. Hilson AJW, Pavia D, Diamond PD, Agnew JE. An ultra-fine ^{99m}Tc-aerosol (Technegas) for lung ventilation scintigraphy: a comparison with ^{81m}Kr [Abstract]. *J Nucl Med* 1989;30:744.
27. Cook G, Clarke SEM. An evaluation of Technegas as a ventilation agent compared with krypton-81m in the scintigraphic diagnosis of pulmonary embolism. *Eur J Nucl Med* 1992;19:770–774.
28. Peltier P, DeFaucal P, Chetanneau A, Chatal J-F. Comparison of technetium-99m aerosol and krypton-81m ventilation studies for the diagnosis of pulmonary embolism. *Nucl Med Commun* 1990;11:631–638.
29. Alderson PO, Biello DR, Gottschalk A, et al. Technetium-99m-DTPA aerosol and radioactive gases compared as adjuncts to perfusion scintigraphy in patients with suspected pulmonary embolism. *Radiology* 1984;153:515–521.
30. Agnew JE, Bateman JRM, Pavia D, Clarke SW. Radionuclide demonstration of ventilatory abnormalities in mild asthma. *Clin Sci* 1984;66:525–531.
31. Scott WR, Taulbee DB. Aerosol deposition along the vertical axis of the lung. *J Aerosol Sci* 1985;16:323–333.
32. Chamberlain MJ, Morgan WDC, Vinitski S. Factors influencing the regional deposition of inhaled particles in man. *Clin Sci* 1983;64:69–78.
33. Line BR. Go with the flow but how far? *J Nucl Med* 1992;33:1939–1942.